Jurnal Fisika
Himpunan Fisika Indonesia
Vol. 10 - No. 2 - Desember 2010

ISSN 0854-3046
Akreditasi: No. 242/Akred-LIPI/P2MBI/05/2010

INFLUENCE OF MILLING TIME ON STRUCTURAL AND MAGNETIC PROPERTIES OF ZnO NANOPARTICLES PREPARED BY MECHANICAL MILLING

K. Tarigan[1,2], M. Ginting[3], V. D. Lam[4], T. D. Thanh[4], D. H. Manh[4], T. L. Phan[1]

[1]Department of Physics, Chungbuk National University, Cheongju 361-763, Korea
[2]Department of Electrical Engineering, Indonesia Institute of Technology, Serpong, Tangerang Selatan 15320, Indonesia
[3]Research and Development Center for Applied Physics, LIPI, Serpong, Tangerang Selatan 15314, Indonesia
[4]Institute of Materials Science, Vietnam Academy of Science and Technology, Hanoi, Vietnam
E-mail: ptlong2512@yahoo.com.

ABSTRACT

Influences of the milling time on structural and magnetic properties of nanocrystalline ZnO samples prepared by mechanical milling process have been studied in detail. Experimental results reveal that with varying the milling time from 1 to 24 hrs the average crystallite size calculated from Scherrer's equation is in the range of 13 - 18 nm. All the samples exhibit the ferromagnetic behavior above room temperature. The ferromagnetic order increased with increasing the milling time. By means of X-ray diffraction analyses and measurements of the magnetization versus temperature, we suggest that the ferromagnetism in ZnO nanoparticles is due to a $Fe_{0.902}O$-related metastable phase, in which Fe impurity is generated from the stainless steel vial wall and balls.

Keywords: ZnO nanoparticles; mechanical milling; X-ray diffraction; magnetism.

ABSTRAK

Pengaruh waktu milling terhadap sifat-sifat struktural dan magnetik sampel nanokristalin ZnO yang dibuat dengan proses milling mekanik telah dipelajari secara rinci. Hasil-hasil eksperimen memperlihatkan, dengan perubahan waktu milling dari 1 ke 24 jam menghasilkan ukuran rata-rata kristalit yang dihitung dengan persamaan Scherrer adalah antara 13 – 18 nm. Semua sampel menunjukkan perilaku feromagnetik di atas suhu kamar. Sifat feromagnetik meningkat mengikuti pertambahan waktu milling. Berdasarkan hasil analisa difraksi sinar-x dan peralatan magnetisasi versus temperature, kami menduga bahwa sifat ferromagnetik dalam nanopartikel ZnO ini berhubungan dengan fase metastabil $Fe_{0.902}O$, di mana impuritas Fe dihasilkan dari dinding stainless steel vial dan bola-bola.

Kata kunci: *ZnO nanoparticles; mechanical milling; X-ray Diffraction; magnetism.*

PACS: 81.05.Dz, 61.46.Hk, 75.75.-c

ISSN 0854-3046
Akreditasi: No. 242/Akred-LIPI/P2MBI/05/2010

INTRODUCTION

Zinc oxide (ZnO) is an inexpensive and highly chemical- and thermal-stable semiconductor compound. It is emerging as a potential material for a variety of applications. In electronic and optoelectronic fields, conductive and transparent natures make ZnO suitable for displays and photovoltaic panels, which can replace for another costly transparent conductor of ITO. With a wide-band gap (3.37 eV) and a large exciton binding energy (60 meV), ZnO is considered as an important material for ultraviolet/blue devices working at room temperature. It has been also used the piezoelectric property of ZnO in some commercial products such as accelerometers, force sensors, pressure sensors, acoustic sensors, and ultrasonic transducers [1, 2]. Particularly, with biocompatibility and no-toxicity it is suitable for personal care applications of sunscreen products, cosmetics (due to ZnO's preeminent behavior in absorbing ultraviolet radiations), and medical creams.

Recently, it has been discovered that ZnO exhibits a variety of novel structures in the nanoscale, including nanoparticles, nanowires, nanotubes, nanocombs, and so forth [2, 3]. This opens up new potential applications in nanoscale electronic and optoelectronic devices [2-8], and biomedical and environmental technologies [9-11]. For example, ZnO nanowires/nanorods can be used in nanogenerators [5, 6] and gas sensors [4]. With the successful growth of *p*-type ZnO nanowires/nanorods, it is expected to fabricate a new generation of inexpensive ZnO-based light-emitting diodes (LEDs) [7, 8]. Concerning ZnO nanoparticles, their applications are widely in many fields, including phosphor powders, photocatalysis, textiles, food additives, pigments, and microorganism [2, 9, 11, 12]. Thus, the fabrication of a large amount of ZnO nanoparticles is always an imperative demand.

Basically, there are two approaches of "bottom-up" and "top-down" to synthesize ZnO nanoparticles. While the former is based on advanced chemical methods (such as the sol-gel technique, aqueous chemical deposition, chemical co-precipitation, *etc.*), the latter is based on the high-energy ball milling (mechanical grinding process) with low-cost production [13]. The starting materials for the mechanical milling are usually micro-sized powders. In the ball-milling operation, there are two processes taking place simultaneously: particle fracturing and cold welding. The powders are plastically deformed under high-energy impacts through ball-to-ball and ball-to-vial wall collisions. The grinding process thus depends on many factors, including temperature, ambient, chemical composition of powder mixtures, grinding tools, and so forth [13, 14].

Because of the capacity in fabricating a large amount of nanoparticles, this method has been used to make ZnO nanoparticles [15-21] as starting from commercial ZnO powders. To fabricate ZnO nanoparticles, milling tools (balls and vials) of zirconium, agate, and stainless-steel are employed. The use of such the milling media, synthesized ZnO nanoparticles are usually adhered by impurities

ISSN 0854-3046
Akreditasi: No. 242/Akred-LIPI/P2MBI/05/2010

generated from balls and vials [17, 20]. However, this situation has not been investigated in detail yet, particularly for ZnO nanoparticles fabricated in the stainless-steel milling medium.

In this work, we report a thorough study of the influences of the milling on the structural and magnetic properties of nanocrystalline ZnO samples prepared by high-energy ball milling in which the stainless-steel vial and balls are used. Our experimental results have proved an existence of a secondary phase generated from the milling medium, which is responsible for ferromagnetism in the samples.

EXPERIMENTAL DETAILS

To make nanoparticles, we used commercial ZnO powders (99.995% purity, and particle diameters of about 200 nm) as the precursor. For each sample, an amount of 3.5 g ZnO powders was loaded in a stainless-steel vial containing five balls (two balls with 10.7 mm diameter, and the others with 4.5 mm diameter). The ball-to-powder ratio was 5:1. Before milling process, we carried out the coating step for 30 minutes to avoid impurity from vial and balls. The milling process was performed at room temperature by 8000D Dual Mixer/Mill (SPEX Sample Prep) in an Ar ambient to avoid air contamination. The milling time (t_m) was varied to be 1, 3, 9, 12, and 24 hrs. This process is shows in Figure 1. For reference, powders clung to the vial wall and balls were scraped to check their properties (this sample was named R). The morphology and particle size of the final samples were examined by a field-emission electron scanning microscope (FE-SEM, Hitachi S-4800). Energy dispersive X-ray (EDX) spectroscopy link with FE-SEM was used to identify impurities present in the samples. The crystal structure was analyzed by an X'Pert Philips diffractometer. The x-ray radiation source was Cu-Kα_1 (λ =1.5406 Å), at applied voltage and current of 40 kV and 30 mA, respectively. Magnetic measurements at room temperature were performed on a superconducting quantum interference device (SQUID), and measurements at high temperatures (above 300 K) were carried out on a vibrating sample magnetometer (VSM).

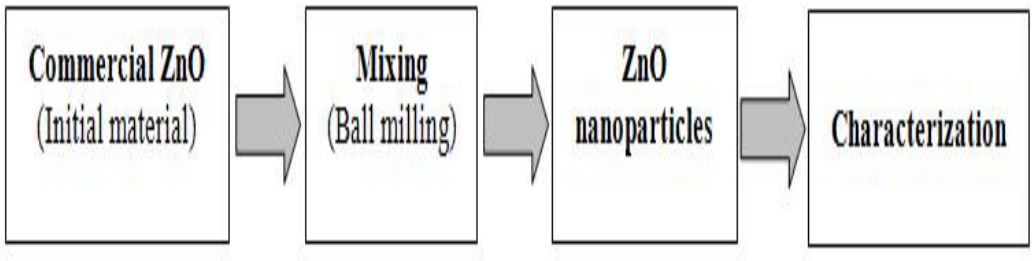

Figure 1. Diagram shows preparation of ZnO nanoparticles.

ISSN 0854-3046
Akreditasi: No. 242/Akred-LIPI/P2MBI/05/2010

RESULTS AND DISCUSSION

Figure 2 shows SEM images of four representative ZnO samples with various milling times of 1, 3, 9, and 24 hrs. One can see that the morphology and size of particles are changed very much when the milling time (t_m) is increased. This is due to the impaction of high energy generated from the ball-to-ball and ball-to-vial wall collisions. For the t_m = 1 hr sample, particle sizes are various in the range of 50 to 200 nm. The t_m increase longer than 9 hrs introduces particles with more homogeneous sizes of about 20 nm. However, these nanoparticles adhere to each other to form clusters with dimensions of 50 - 100 nm, see Figs. 2(c and d). Having used EDX spectroscopy linked with SEM, we find Fe impurity present in the nanocrystalline ZnO samples, see Figure 3.

This impurity is generated from the stainless steel balls and vial wall. Its concentration increases with increasing t_m, and is estimated to be about 0.4 - 1.2 wt%. For a longer milling time of t_m = 100 hrs, Glushenkov *et al*. [17] also found their nanocrystalline ZnO samples containing 6.7 wt% Fe and 1.3 wt% Cr. The absence of Cr impurity in our samples could be due to the fact that the milling time is short or its concentration is too low, which is not detected by EDX spectroscopy.

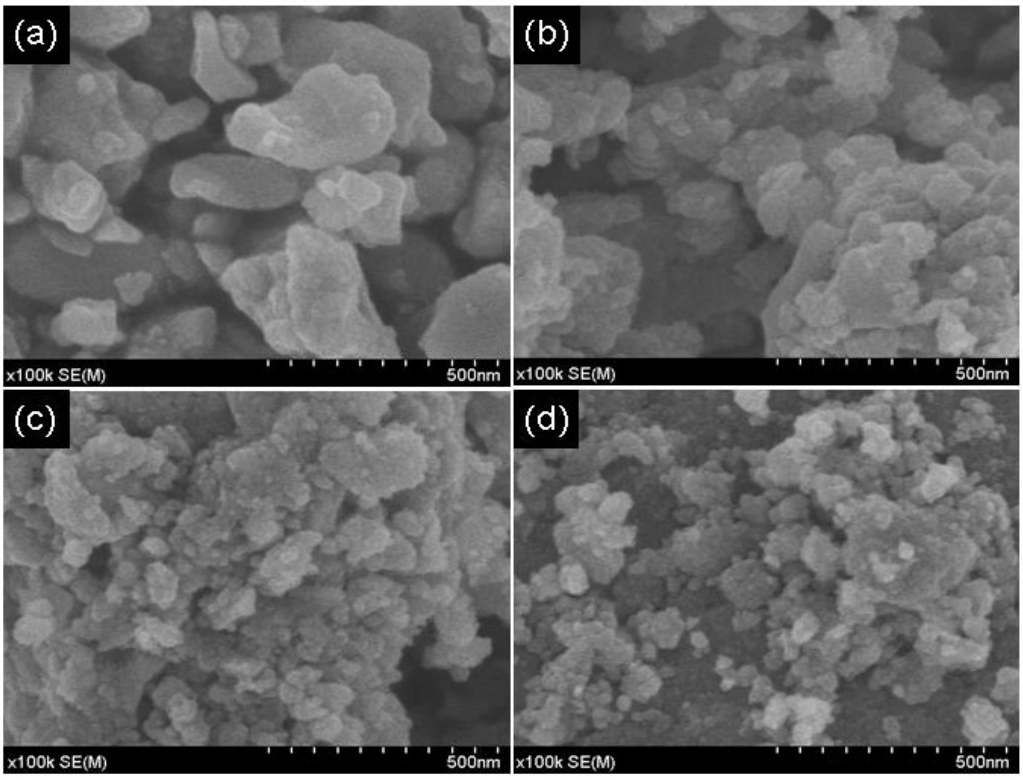

Figure 2. FE-SEM images for ZnO nanoparticle samples with the milling times of (a) 1 hr, (b) 3 hrs, (c) 9 hrs, and (d) 24 hrs.

ISSN 0854-3046
Akreditasi: No. 242/Akred-LIPI/P2MBI/05/2010

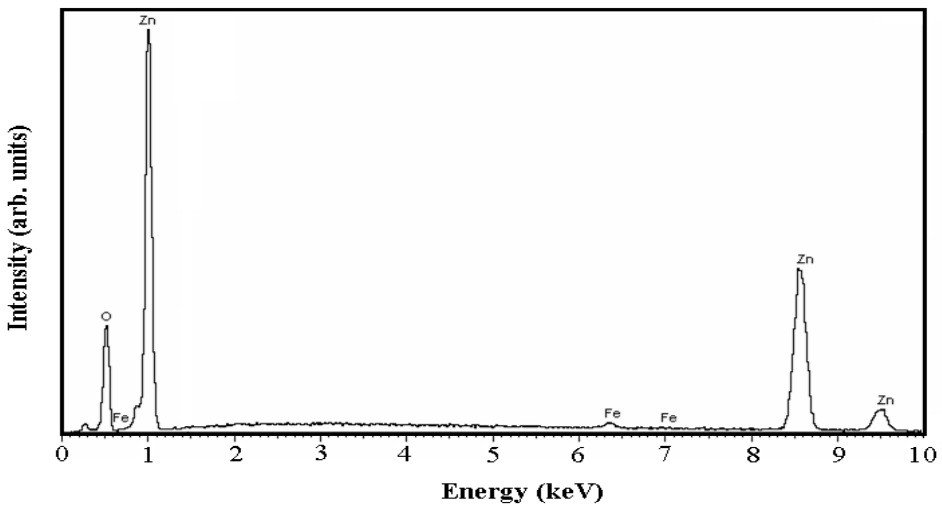

Figure 3. EDX spectrum for the sample with t_m = 12 hrs showing the presence of Fe impurity besides Zn and O.

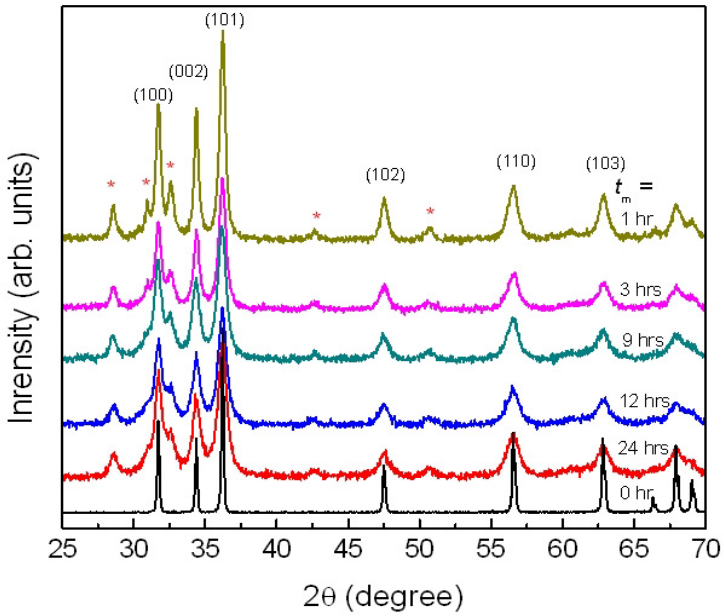

Figure 4. XRD patterns for the nanocrystalline ZnO samples with various milling times in comparison to the as-received ZnO powders (0 hr). Asterisks shows a $Fe_{0.902}O$-related secondary.

To examine structural characterization, we have based on an x-ray diffractometer. Figure 4 shows x-ray diffraction (XRD) patterns of the samples with various milling times. Having compared to the as-received ZnO sample (t_m = 0 hr) corresponding with the indexed XRD peaks, one can see that there is no shift of peak positions for the milled powders. This reflects that the nanocrystalline samples are stable in the wurtzite-type structure. The lattice parameters determined are a = 3.26 and c = 5.22 Å,

ISSN 0854-3046
Akreditasi: No. 242/Akred-LIPI/P2MBI/05/2010

and seem independent of t_m. The t_m increase only causes the weakening and broadening of the diffraction peaks, indicating a disordered crystalline structure and small grain size. In fact, ZnO is a brittle material.

During milling, the local heating effect appearing at contact points of the ball-to-ball and ball-to-vial wall causes plastic deformation of ZnO powders. The decrease in grain/crystallite size is hence completely possible. In an attempt to obtain the crystallite size (D), we used the Scherrer formula [22]:

$$D = \frac{K\lambda}{\beta \cos\theta}, \qquad (1)$$

where β is the FWHM, K is a constant (= 0.89), λ is the x-ray wavelength, and θ is the Bragg angle. For each sample we calculated D for all the indexed peaks, and then took their average value. The results obtained are shown in Figure 5. It appears that D slightly decreases from about 18.5 nm for the t_m = 1 hr sample to 13.5 nm for the t_m = 12 hrs sample. In our case, the value with D = 13.5 nm is considered as a critical size that the t_m increase up to 24 hrs does not further reduce D. Such the tendency is in good agreement with SEM data shown in Figure 2. It is different from previous works that employed a similar milling medium [17, 18], the XRD patterns of our samples exhibit extra peaks besides the main peaks from the wurtzire ZnO, see asterisks in Figure 4. These extra peaks match well with those of the $Fe_{0.902}O$-wuestite structure (the space group: $Pm\bar{3}m$). Here, Fe impurity is generated from the stainless steel vial wall and balls. Under high energy of the milling operation together with the presence of oxygen in the vial, the $Fe_{0.902}O$ phase is constituted. Its XRD peaks are also widened as increasing t_m, revealing that $Fe_{0.902}O$ is in nano-size. However, a question about the position of this phase in the samples (*i.e.*, it coated on ZnO nanoparticles and/or distributed as separate particles) is still a challenge, which warrants further study.

Following structural investigations, we have studied magnetic properties. Figure 6 shows the field dependences of magnetization (*M-H*) for the samples with various milling times and for sample R. The sample denoted R is powders clung to the vial wall and balls, see the experimental part. These data were recorded at 300 K by SQUID. All the samples exhibit the ferromagnetic behavior. Among these, sample R (is nanoparticles scraped from the balls and vial wall) has the greatest magnetization.

Meanwhile, for the others the ferromagnetic order increases with increasing t_m. Particularly, the *M-H* curves attain to saturation values at applied fields beyond ±3 kOe. From these data, we determined values of the saturation magnetization M_s and the coercivity H_c with respect to t_m, as graphed in Figure 7. Both M_s and H_c increase gradually when t_m is increased from 1 to 24 hrs.

ISSN 0854-3046
Akreditasi: No. 242/Akred-LIPI/P2MBI/05/2010

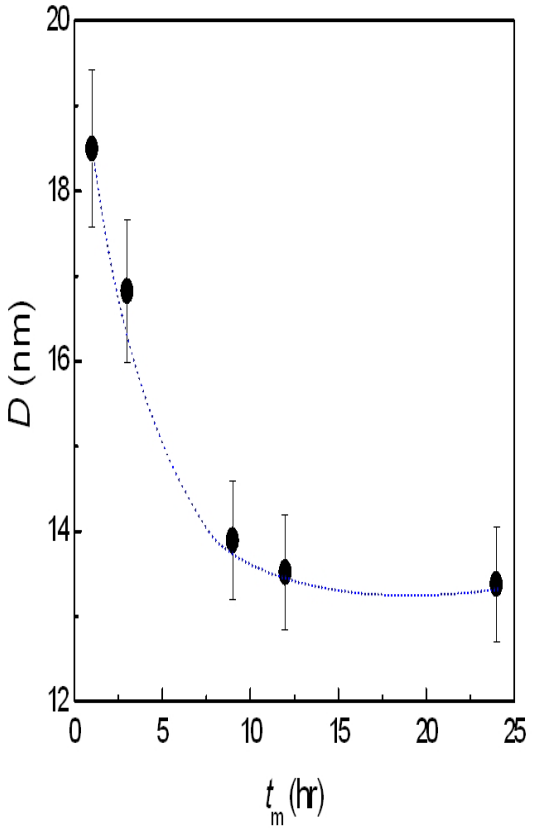

Figure 5. The t_m dependence of the average crystallite size (D) for nanocrystalline ZnO samples. The dotted line is to guide the eye only. Error bars of 5 % are shown.

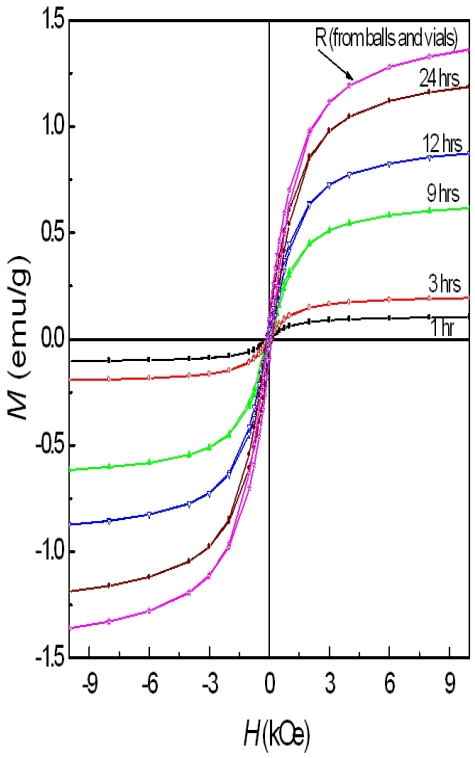

Figure 6. Hysterisis loops for the nanocrystalline ZnO samples with various milling times recorded at 300 K.

For the t_m = 24 hrs sample, M_s and H_c values are about 0.96 emu/g and 120 Oe, respectively. These values are much greater than those determined from other ZnO-based materials, as reviewed in Chapter 5 of Ref. [23].

To gain more insight into the magnetic properties of the system, we have chosen two representative samples of R and t_m = 12 hrs for magnetic measurements at temperatures above 300 K by using VSM. Notice that during the measurement, the samples are put in an Ar ambient to avoid contamination from air. Figure 8 shows temperature dependences of magnetization (M-T) for these samples, which were measured under heating and cooling conditions named MT1 and MT2, respectively.

ISSN 0854-3046
Akreditasi: No. 242/Akred-LIPI/P2MBI/05/2010

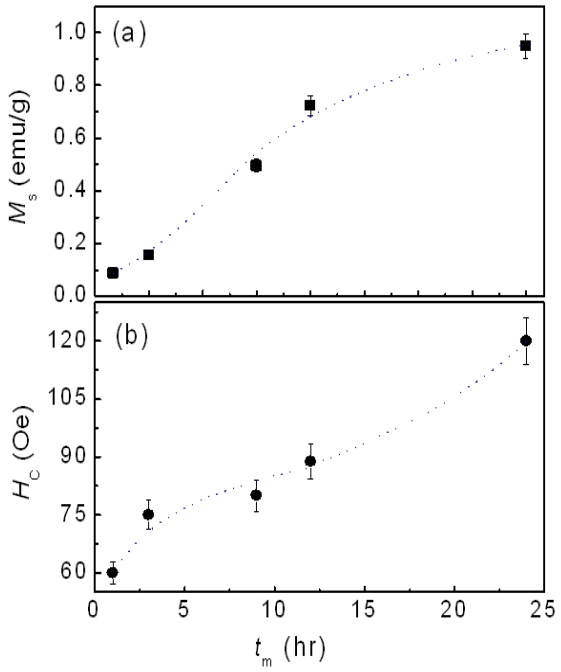

Figure 7. Dependences of (a) M_s and (b) H_c on t_m for the nanocrystalline ZnO samples (dotted lines are to guide the eye only).

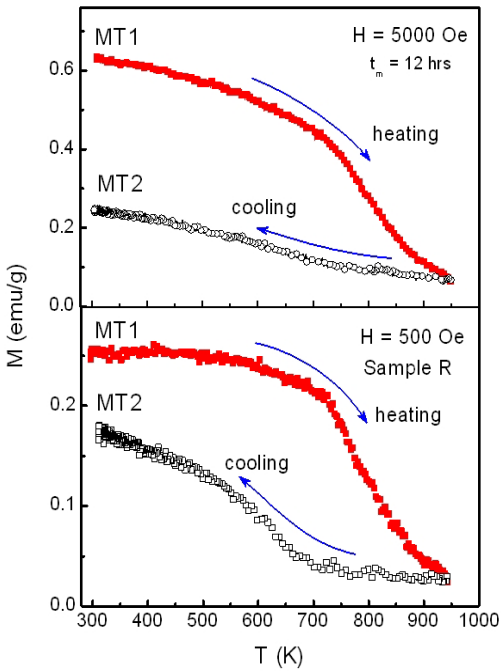

Figure 8. Temperature dependences of magnetization for the samples t_m = 12 hrs and R measured under the heating (MT1) and cooling (MT2) conditions.

The crystallization of metastable nanoparticles leads to the separation of these two curves. The variation tendency of the *M-H* curves for the samples is very similar. This reflects the samples having the same ferromagnetic nature/origin. Concerning the heating process MT1, the ferromagnetic-paramagnetic (FM-PM) phase transition takes place at $T_{C1} \approx 850$ K. In contrast, the measurement according to the cooling process MT2 introduces the FM-PM phase transition at $T_{C2} \approx 600$ K. The separation between two curves MT1 and MT2 is about 0.4 emu/g for the t_m = 12 hrs sample, and 0.1 for sample R. Such the features indicate that the nanocrystalline samples are metastable. If we re-measure *M-T* on these samples following the heating direction once again, the curves recorded will coincides with their MT2 curves.

The above phenomena can be explained as follows: the nanocrystalline samples after ball milling usually contain a high density of lattice defects and grain boundaries. The binding between atoms located at gain boundaries and surfaces is thus weak, which is broken easily by thermal energy due to the heating from 300 to 950 K as measuring MT1. As a result, weakly bound atoms can be evaporated, and the quality of nanoparticles will be improved remarkably, because of defect annihilation and structural reorganization [17]. When the samples are cooled down from 950 K to measure MT2, the crystallization in nanoparticles takes place. There is a transformation from the

ISSN 0854-3046
Akreditasi: No. 242/Akred-LIPI/P2MBI/05/2010

metastable state to the stable state, and the crystallite size can be also increased. Another possibility is that the heating at high temperatures can also causes changes in the composition of ZnO nanoparticles and the secondary phase $Fe_{0.902}O$; *i.e.*, Fe can diffuse into ZnO crystals, and in contrast Zn can diffuse into $Fe_{0.902}O$. Such the circumstances lead to a difference between two curves MT1 and MT2, as can be seen in Figure 8. Regarding to a question of the nature of the ferromagnetism, we have paid attention to the XRD and EDX data. To the limit of the experimental tools, only three elements of Zn, O and Fe are found in our samples corresponding to structural phases of ZnO and $Fe_{0.902}O$. Among these, Zn^{2+} and O^{2-} are nonmagnetic ions, and commercial ZnO powders is known as a diamagnetic material [19, 24].

Recently, Sanyal *et al.* [19] have reported that ZnO nanoparticles fabricated by mechanical milling also exhibits diamagnetic behavior. For the case of the ferromagnetism in ZnO materials caused by lattice defects, M_s values are usually very small, in the range of 1×10^{-5} - 1×10^{-2} emu/g [24-27]. Meanwhile, large values of $M_s \approx 0.1$ - 1.0 emu/g are gained from our samples, see Figs. 7 and 8. With these results, the ferromagnetism in our samples is definitely generated from a Fe-related secondary phase. Having compared to the magnetic behavior of iron and iron oxides shown in Table 1, compounds Fe, FeO, Fe_2O_3, $ZnFe_2O_4$ (both normal and inverse spinel structures), and $(Zn, Fe)_3O_4$ can not be responsible for the ferromagnetism because their magnetic phase transition temperature (the Curie temperature or the Néel temperature) is far from that of our samples.

There is only Fe_3O_4 with $T_C \approx 858$ K very close to the value $T_C \approx 850$ K of our nanoparticles. However, the XRD data in Figure 3 do not indicate its existence. We believe that the ferromagnetism

Table 1. Magnetic properties of some secondary phases related to iron and iron oxides.

Phase	Magnetic nature	Curie temperature or Néel temperature (K)	Reference
$Fe_{0.902}O$ (nanocrystalline, cubic)	Ferromagnetic	~850	Present work
Fe	Ferromagnetic	1043	[28]
FeO (cubic)	Antiferromagnetic	198	[28]
Fe_2O_3	Ferromagnetic	948	[29]
Fe_3O_4	Ferromagnetic	858	[28]
$(Zn, Fe)_3O_4$	Ferromagnetic	440	[23]
$ZnFe_2O_4$ (bulk, normal spinel)	Nonmagnetic	-	[23]
$ZnFe_2O_4$ (nanocrystalline, inverse spinel)	Ferrimagnetic	-	[23]

ISSN 0854-3046
Akreditasi: No. 242/Akred-LIPI/P2MBI/05/2010

in the samples is caused by wuestite $Fe_{0.902}O$. It also appears in nanosizes and is metastable, similar to ZnO nanoparticles. The enhancement in ferromagnetic order is a consequence of development of this phase when t_m is increased. For sample R, nanoparticles cling directly to the milling media for a long time, the magnetization is thus highest.

CONCLUSION

We used the mechanical milling to prepare ZnO nanoparticles, started from commercial ZnO powders. The variation of the milling time t_m from 1 to 24 hrs reduced the crystallite size D to about 13.5 nm. The EDX and XRD studies revealed the presence of Fe impurity generated from the grinding vial wall and balls. Under high energy of the milling operation this impurity constituted $Fe_{0.902}O$ with the wuestite-type structure, which was responsible to the high-temperature ferromagnetism in ZnO nanoparticles. The t_m increase would enhance the impurity level, and thus resulted in the increase in the ferromagnetic order. Notably, ZnO nanoparticles prepared by the mechanical milling are metastable, and there is the crystallization when they are cooled from high temperatures.

REFERENCES

1. Arora, A., P. J. George, A. Arora, V. K. Dwivedi and V. Gupta. *Sensors & Transducers Journal 91* (2008): 70.
2. Jagadish, C., and S. J. Pearton. "Zinc oxide bulk." *Thin Films and Nanostructures,* Elsevier, 2006.
3. Wang, Z.L. *Journal of Physics: Condensed Matter 16* (2004): R828.
4. Liao, L., H. B. Lu, M. Shuai, J. C. Li, Y. L. Liu, C. Liu, Z. X. Shen and T. Yu. *Nanotechnology 19* (2008): 175501.
5. Qin, Y., X. D. Wang and Z. L. Wang. *Nature 451* (2008): 809.
6. Wang, Z.L., and J. H. Song. *Science 312* (2006): 242.
7. Xiang, B., P. W. Wang, X. Z. Zhang, S. A. Dayeh, D. P. R. Aplin, C. Soci, D. P. Yu and D. L. Wang. *Nano Letter 7* (2007): 323.
8. Yuan, G.D., W. J. Zhang, J. S. Jie, X. Fan, J. A. Zapien, Y. H. Leung, L. B. Luo, P. F. Wang, C. Lee, S., and S. T. Lee. *Nano Letter 8* (2008): 2591.
9. Brayner, R., S. A. Dahoumane, C. Yepremian, C. Djediat, M. Meyer, A. Coute and F. Fievet. *Langmuir 26* (2010): 6522.
10. Chu, D.W., Y. Masuda, T. Ohji and K. Kato. *Langmuir 26* (2010): 2811.
11. N. Padmavathy, N., and R. Vijayaraghavan. *Science and Technology Advanced Materials 9* (2008): 035004.
12. Kathirvelu, S., D. S. Louis and B. Dhurai. *Indian Journal of Fibre and Textile Research 34* (2009): 267.

ISSN 0854-3046
Akreditasi: No. 242/Akred-LIPI/P2MBI/05/2010

13. Suryanarayana,C. *Progress in Materials Science 46* (2001): 1.
14. Bégin-Colin, S., T. Girot, G. Le Caër and A. Mocellin. *Journal of Solid State Chemistry 149* (2000): 41.
15. Damonte, L.C., L. A. Mendoza Zélis, B. Marí Soucase and M. A. Hernández Fenollosa. *Powder Technology 148* (2004): 15.
16. Dutta, S., S. Chattopadhyay, M. Sutradhar, A. Sarkar, M. Chakrabarti, D. Sanyal and D. Jana. *Journal of Physics: Condensed Matter 19* (2007): 236218.
17. Glushenkov, A.M., H. Z. Zhang, J. Zou, G. Q. Lu and Y. Chen. *Nanotechnology 18* (2007): 175604.
18. Lemine, O.M., A. Alyamani and M. Bououdina. *International Journal of Nanotechnology and Applications 2* (2008): 161.
19. Sanyal, D., T. K. Roy, M. Chakrabarti, S. Dechoudhury, D. Bhowmick and A. Chakrabarti. *Journal of Physics: Condensed Matter 20* (2008): 045217.
20. Vojisavljevic, K., M. Scepanovic, T. Sreckovic, M. Grujic-Brojcin, Z. Brankovic and G. Brankovic. *Journal of Physics: Condensed Matter 20* (2008): 475202.
21. Sreckovic, T., S. Bernik, M. Ceh and K. Vojisavljevic. *Journal of Microscopy 232* (2008): 639.
22. Waren, B.E. *X-ray diffraction: Reading*, MA: Addison-Wesley, 1969.
23. Morkoc, H., and U. Ozgur. "Zinc Oxide: Fundamentals." *Materials and Device Technology,* Weinheim: WILEY-VCH Verlag GmbH & Co. KGaA, 2009.
24. Hong, N.H. *Magnetism in Semiconducting Oxides,* Transword Research Network, 2007.
25. Phan, T.L., and S. C. Yu. *Journal of the Korean Physical Society 56* (2010): 1160.
26. Sundaresan, A., R. Bhargavi, N. Rangarajan, U. Siddesh and C. N. R. Rao. *Review B 74* (2006): 161306.
27. Straumal, B.B., A. A. Mazilkin, S. G. Protasova, A. A. Myatiev, P. B. Straumal, G. Schütz, P. A. van Aken, E. Goering and B. Baretzky. *Physical Review B 79* (2009): 205206.
28. Kittel, C. *Introduction to Solid State Physics*, John Willey & Sons, 2005.
29. Lowrie, W. *Fundamentals of Geophysics,* Cambridge: Cambridge University Press, 1997.